Open Journal of Fluid Dynamics, 2011, 1, 1-11
doi:10.4236/ojfd.2011.11001 Published Online December 2011 (http://www.SciRP.org/journal/ojfd)

Radiation Effect on Natural Convection near a Vertical Plate Embedded in Porous Medium with Ramped Wall Temperature

Sanatan Das, Mrinal Jana, Rabindra Nath Jana
Department of Applied Mathematics, Vidyasagar University, Midnapore, India
E-mail: jana261171@yahoo.co.in
Received November 16, 2011; revised December 7, 2011; accepted December 20, 2011

Abstract

Radiation effect on the natural convection flow of an optically thin viscous incompressible fluid near a vertical plate with ramped wall temperature in a porous medium has been studied. The exact solution of momentum and energy equations is obtained by the use of Laplace transform technique. The variations in fluid velocity and temperature are shown graphically whereas the numerical values of shear stress and the rate of heat transfer at the wall are presented in tabular form for various values of flow parameters. The results show that the fluid velocity increases with increase in Grashof number, Darcy number and time parameters whereas the fluid velocity decreases with increase in the radiation parameter and Prandtl number for ramped temperature as well as isothermal wall temperature. It is found that an increase in radiation parameter leads to rise the temperature for both ramped wall temperature as well as isothermal wall temperature. Further, it is found that an increase in Prandtl number leads to fall the temperature for both ramped wall temperature as well as isothermal wall temperature. The shear stress at the wall decreases with increases in either Prandtl number or porosity parameter while the result shows reverse in the case of radiation parameter. Finally, the rate of heat transfer is increased with increase in the radiation parameter for both ramped wall temperature as well as isothermal wall temperature.

Keywords: Natural Convection, Darcy Number, Radiation Parameter, Prandtl Number, Porous Medium, Ramped Wall Temperature and Isothermal Wall Temperature

1. Introduction

The phenomenon of natural convection arises in fluids when temperature changes cause density variations leading to buoyancy forces acting on the fluid particles. Such flows which are driven by temperature differences abound in nature and have been studied extensively because of its applications in engineering, geophysical and astrophysical environments. Comprehensive literature on various aspects of free convection flows and its applications could be found in Ghoshdastidar [1], Nield and Bejan [2]. Ghoshdastidar gave various areas of applications of free convection flow such as those found in heat transfer from pipes and transmission lines as well as from electronic devices, heat dissipation from the coil of a refrigerator unit to the surrounding air, heat transfer from a heater to room air, heat transfer in nuclear fuel rods to the surrounding coolant, heated and cooled enclosures, quenching, wire-drawing and extrusion, atmospheric and oceanic circulation. Unsteady free convection flows in a porous medium have received much attention in recent time due to its wide applications in geothermal and oil reservoir engineering as well as other geophysical and astrophysical studies. Moreover, considerable interest has been shown in radiation interaction with convection for heat and mass transfer in fluids. This is due to the significant role of thermal radiation in the surface heat transfer when convection heat transfer is small, particularly in free convection problems involving absorbing-emitting fluids. The unsteady fluid flow past a moving plate in the presence of free convection and radiation were studied by Mansure [3], Raptis and Perdikis [4], Das *et al.* [5], Grief *et al.* [6], Ganeasan and Loganathan [7], Mbeledogu *et al.* [8], Makinde [9] and Abdus-Sattar and Hamid Kalim [10]. All these studies have been confined to unsteady flow in a non-porous medium.

Israel-Cookey *et al.* [11] have studied the influence of viscous dissipation and radiation on unsteady MHD free-convection flow past an infinite heated vertical plate in a porous medium with time-dependent suction. Radiative and free convective effects of a MHD flow through a porous medium between infinite parallel plates with time dependent suction have been investigated by Alagoa *et al.* [12]. Israel-Cookey *et al.* [13] have made an analysis on MHD oscillatory Couette flow of a radiating viscous fluid in a porous medium with periodic wall temperature. Sattar and Maleque [14,15] have studied the unsteady MHD Natural convection flow and mass transfer along an accelerated porous plate in a porous medium. Thermal radiation interaction with unsteady MHD flow past a vertical porous plate immersed in a porous medium has been analyzed by Samad and Rahman [16]. Mahanti and Gaur [17] have studied the effects of varying viscosity and thermal conductivity on steady free convective flow and heat transfer along an isothermal vertical plate in the presence of heat sink. Transient free convection past a semi-infinite vertical plate with variable surface temperature has been investigated by Takhar *et al.* [18].

In this present paper, we investigate the effects of radiation on the free convection flow of an optically thin incompressible viscous fluid past an infinite vertical plate with ramped wall temperature in porous medium. The fluid considered is a gray, radiation, absorbing, emitting but non-scattering medium and the Rosseland approximation is used to describe the radiative heat transfer in the energy equation. It is seen that the velocity u_1 decreases for both ramped wall temperature as well as isothermal wall temperature with an increase in either radiation parameter Ra or Prandtl number Pr. It is also seen that the velocity u_1 increases for both ramped wall temperature as well as isothermal wall temperature with an increase in either Grashof number Gr or time τ. It is found that an increase in radiation parameter Ra leads to rise the temperature θ for both ramped wall temperature as well as isothermal wall temperature. Further, it is found that an increase in Prandtl number leads to fall the temperature for ramped temperature as well as isothermal case.

2. Formulation of the Problem and Its Solutions

Consider the unsteady free convection flow of an optically thin viscous incompressible fluid past an moving infinite vertical plate coinciding with plane $y=0$, where the flow is confined to $y>0$ in a porous medium. Choose a cartesian co-ordinates system with *x*-axis along the wall in a vertically upward direction and *y*-axis is normal to it into the fluid (see **Figure 1**). At $t \le 0$, the plate and the surrounding fluid are at the same constant temperature T_∞. At time $t>0$, the temperature of the wall is raised or lowered to $T_\infty + (T_w - T_\infty)\dfrac{t}{t_0}$ when $0<t\le t_0$ and the constant temperature T_w is maintained at $t>t_0$. Since the plate is infinite along *x*-direction, all the physical variables are the function of y and t only. The flow is considered optically thin gray gas with natural convection and radiation. The radiative heat flux in the *x*-direction is considered negligible in comparison to *y*-direction.

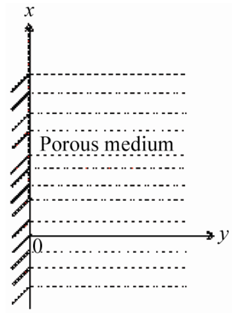

Figure 1. Geometry of the problem.

The Boussinesq approximation is assumed to hold and for the evaluation of the gravitational body force, the density is assumed to depend on the temperature according to the equation of reference state

$$\rho = \rho_0\left[1-\beta^*\left(T-T_\infty\right)\right], \tag{1}$$

where T is the fluid temperature, ρ the fluid density, β^* the coefficient of thermal expansion and T_∞ and ρ_0 being the reference temperature and the density respectively.

Using Boussinesq Approximation (1), the momentum equation in a porous medium along *x*-axis is

$$\frac{\partial u}{\partial t} = \nu\frac{\partial^2 u}{\partial y^2} + g\beta^*\left(T-T_\infty\right) - \frac{\nu}{k^*}u, \tag{2}$$

where u, g, β^*, ν, ρ and k^* are respectively, fluid velocity, acceleration due to gravity, coefficient of thermal expansion, kinematic viscosity, fluid density and permeability of a porous media.

The energy equation is

$$\frac{\partial T}{\partial t} = \frac{k}{\rho c_p}\frac{\partial^2 T}{\partial y^2} - \frac{1}{\rho c_p}\frac{\partial q_r}{\partial y}, \tag{3}$$

where k is the thermal conductivity, c_p the specific heat at constant pressure and q_r the radiative heat flux.

The initial and boundary conditions are

$$u=0,\ T=T_\infty \ \text{ for } \ y\ge 0 \ \text{ and } \ t\le 0,$$
$$u=U_0 \ \text{ at } \ y=0 \ \text{ for } \ t>0,$$

$$T = T_\infty + \left(T_w - T_\infty\right)\frac{t}{t_0} \quad \text{at } y = 0 \text{ for } 0 < t \le t_0$$
$$T = T_w \quad \text{at } y = 0 \text{ for } t > t_0 \tag{4}$$
$$u \to 0, T \to T_\infty \quad \text{as } y \to \infty \text{ for } t > 0$$

It has been shown by Cogley *et al.* [19] that in the optically thin limit for a non-gray gas near equilibrium, the following relation holds

$$\frac{\partial q_r}{\partial y} = 4\left(T - T_\infty\right)\int_0^\infty K_{\lambda_0}\left(\frac{\partial e_{\lambda h}}{\partial T}\right)_0 \mathrm{d}\lambda, \tag{5}$$

where K_λ is the absorption coefficient, λ is the wave length, $e_{\lambda h}$ is the Plank's function and subscript `0′ indicates that all quantities have been evaluated at the temperature T_∞ which is the temperature of the wall at time $t \le 0$. Thus our study will be limited to small difference of wall temperature to the fluid temperature.

On the use of (5), Equation (3) becomes

$$\frac{\partial T}{\partial t} = \frac{k}{\rho c_p}\frac{\partial^2 T}{\partial y^2} - \frac{4}{\rho c_p}\left(T - T_\infty\right)I, \tag{6}$$

where

$$I = \int_0^\infty K_{\lambda_0}\left(\frac{\partial e_{\lambda h}}{\partial T}\right)_0 \mathrm{d}\lambda. \tag{7}$$

Introducing dimensionless variables

$$\eta = \frac{y}{U_0 t_0}, \quad \tau = \frac{t}{t_0}, \quad u_1 = \frac{u}{U_0}, \quad \theta = \frac{T - T_\infty}{T_w - T_\infty}, \tag{8}$$

Equations (2) and (6) become

$$\frac{\partial u_1}{\partial \tau} = \frac{\partial^2 u_1}{\partial \eta^2} - \frac{1}{\sigma}u_1 + Gr\theta, \tag{9}$$

$$\frac{\partial \theta}{\partial \tau} = \frac{1}{\Pr}\frac{\partial^2 \theta}{\partial \eta^2} - Ra\theta, \tag{10}$$

where $Gr = \dfrac{g\beta^* \nu\left(T_w - T_\infty\right)}{U_0^3}$ is Grashof number, $\Pr = \dfrac{\nu \rho c_p}{k}$ the Prandtl number, $Ra = \dfrac{4I\nu}{\rho c_p U_0^2}$ the radiation parameter, $\sigma = \dfrac{k^* U_0^2}{\nu^2} = MaDa$ the porosity parameter and Da the Darcy number.

The characteristic time t_0 is defined as

$$t_0 = \frac{\nu}{U_0^2}. \tag{11}$$

The corresponding initial and boundary conditions for u_1 and θ are

$$u_1 = 0, \theta = 0 \quad \text{for } \eta \ge 0 \text{ and } \tau \le 0,$$
$$u_1 = 1 \quad \text{at } \eta = 0 \text{ for } \tau > 0,$$
$$\theta = \tau \quad \text{at } \eta = 0 \text{ for } 0 < \tau \le 1, \tag{12}$$
$$\theta = 1 \text{ at } \eta = 0 \text{ for } \tau > 1, \; u_1 \to 0,$$
$$\theta \to 0 \text{ as } \eta \to \infty \text{ for } \tau > 0.$$

Taking Laplace transformation of the Equations (9) and (10), we get

$$\frac{\mathrm{d}^2 \bar{u}_1}{\mathrm{d}\eta^2} - \left(s + \frac{1}{MaDa}\right)\bar{u}_1 = -Gr\bar{\theta}, \tag{13}$$

$$\frac{\mathrm{d}^2 \bar{\theta}}{\mathrm{d}\eta^2} - \Pr\left(s + Ra\right)\bar{\theta} = 0, \tag{14}$$

where

$$\bar{u}_1\left(\eta, s\right) = \int_0^\infty u_1\left(\eta, \tau\right)e^{-s\tau}\mathrm{d}\tau,$$
$$\bar{\theta}\left(\eta, s\right) = \int_0^\infty \theta\left(\eta, \tau\right)e^{-s\tau}\mathrm{d}\tau. \tag{15}$$

The corresponding boundary conditions for $\bar{u}_1$ and $\bar{\theta}$ are

$$\bar{u}_1 = \frac{1}{s}, \bar{\theta} = \frac{1}{s^2}\left(1 - e^{-s}\right) \text{ at } \eta = 0,$$
$$\bar{u}_1 \to 0, \bar{\theta} \to 0 \text{ as } \eta \to \infty. \tag{16}$$

The solution of the Equations (14) and (13) subject to the boundary conditions (16) can be easily obtained and are given by

$$\bar{\theta}\left(\eta, s\right) = \frac{\left(1 - e^{-s}\right)}{s^2}e^{-\eta\sqrt{\Pr(s+Ra)}}, \tag{17}$$

$$\bar{u}_1\left(\eta, s\right) = \frac{1}{s}e^{-\eta\sqrt{s+\frac{1}{MaDa}}} - \frac{\alpha\left(1 - e^{-s}\right)}{s^2(s-\beta)}\left[e^{-\eta\sqrt{s+\frac{1}{MaDa}}} - e^{-\eta\sqrt{\Pr(s+Ra)}}\right] \tag{18}$$

where

$$\alpha = \frac{Gr}{\left(1 - \Pr\right)} \text{ and } \beta = \frac{\left(\Pr Ra - \frac{1}{MaDa}\right)}{\left(1 - \Pr\right)}. \tag{19}$$

Taking the inverse Laplace transform of Equations (17) and (18), the solution for the fluid temperature $\theta\left(\eta, \tau\right)$ and fluid velocity $u_1\left(\eta, \tau\right)$ are obtained and are given by

$$\theta\left(\eta, \tau\right) = \theta_1\left(\eta, \tau\right) - \theta_1\left(\eta, \tau - 1\right)H\left(\tau - 1\right), \tag{20}$$

$$u_1\left(\eta, \tau\right) = \frac{1}{2}\left[e^{\frac{\eta}{\sqrt{MaDa}}}\operatorname{erfc}\left(\frac{\eta}{2\sqrt{\tau}} + \sqrt{\frac{\tau}{MaDa}}\right) + e^{-\frac{\eta}{\sqrt{MaDa}}}\operatorname{erfc}\left(\frac{\eta}{2\sqrt{\tau}} - \sqrt{\frac{\tau}{MaDa}}\right)\right]$$

$$-\alpha\left[\phi_1(\eta,\tau)-\phi_1(\eta,\tau-1)H(\tau-1)\right], \quad (21)$$

where

$$\theta_1(\eta,\tau)=\frac{1}{2}\left[\left(\tau+\frac{\eta}{2}\sqrt{\frac{\Pr}{Ra}}\right)e^{\eta\sqrt{\Pr Ra}}\times\operatorname{erfc}\left(\frac{\eta}{2}\sqrt{\frac{\Pr}{\tau}}+\sqrt{Ra\tau}\right)+\left(\tau-\frac{\eta}{2}\sqrt{\frac{\Pr}{Ra}}\right)e^{-\eta\sqrt{\Pr Ra}}\operatorname{erfc}\left(\frac{\eta}{2}\sqrt{\frac{\Pr}{\tau}}-\sqrt{Ra\tau}\right)\right], \quad (22)$$

$$\begin{aligned}\phi_1(\eta,\tau)=\frac{1}{2}\Bigg[&\frac{e^{\beta\tau}}{\beta^2}\Bigg\{e^{\eta\sqrt{\frac{1}{MaDa}+\beta}}\times\operatorname{erfc}\left(\frac{\eta}{2\sqrt{\tau}}+\sqrt{\left(\frac{1}{MaDa}+\beta\right)\tau}\right)+e^{-\eta\sqrt{\frac{1}{MaDa}+\beta}}\operatorname{erfc}\left(\frac{\eta}{2\sqrt{\tau}}-\sqrt{\left(\frac{1}{MaDa}+\beta\right)\tau}\right)\\&-e^{\eta\sqrt{\Pr(Ra+\beta)}}\operatorname{erfc}\left(\frac{\eta}{2}\sqrt{\frac{\Pr}{\tau}}+\sqrt{(Ra+\beta)\tau}\right)-e^{-\eta\sqrt{\Pr(Ra+\beta)}}\operatorname{erfc}\left(\frac{\eta}{2}\sqrt{\frac{\Pr}{\tau}}-\sqrt{(Ra+\beta)\tau}\right)\Bigg\}\\&-\frac{1}{\beta}\left(\tau+\frac{1}{\beta}+\frac{\eta\sqrt{MaDa}}{2}\right)e^{\frac{\eta}{\sqrt{MaDa}}}\times\operatorname{erfc}\left(\frac{\eta}{2\sqrt{\tau}}+\sqrt{\frac{\tau}{MaDa}}\right)\\&-\frac{1}{\beta}\left(\tau+\frac{1}{\beta}-\frac{\eta\sqrt{MaDa}}{2}\right)e^{-\frac{\eta}{\sqrt{MaDa}}}\times\operatorname{erfc}\left(\frac{\eta}{2\sqrt{\tau}}-\sqrt{\frac{\tau}{MaDa}}\right)+\frac{1}{\beta}\left(\tau+\frac{1}{\beta}+\frac{\eta}{2}\sqrt{\frac{\Pr}{Ra}}\right)e^{\eta\sqrt{\Pr Ra}}\\&\times\operatorname{erfc}\left(\frac{\eta}{2}\sqrt{\frac{\Pr}{\tau}}+\sqrt{Ra\tau}\right)+\frac{1}{\beta}\left(\tau+\frac{1}{\beta}-\frac{\eta}{2}\sqrt{\frac{\Pr}{Ra}}\right)\times e^{-\eta\sqrt{\Pr Ra}}erfc\left(\frac{\eta}{2}\sqrt{\frac{\Pr}{\tau}}-\sqrt{Ra\tau}\right)\Bigg],\end{aligned} \quad (23)$$

where $\operatorname{erfc}(x)$ is the complementary error function and $H(\tau-1)$ is the unit step function.

2.1. Solution in Case of Unit Prandtl Number

Prandtl number is a measure of the relative strength of the viscosity and thermal conductivity of the fluid. So the case $\Pr=1$ corresponds to those fluids for which both viscous and thermal boundary layer thickness are of the same order of magnitude. Setting $\Pr=1$ in Equation (14) and following the same procedure as before, the exact solution for the fluid temperature $\theta(\eta,\tau)$ and fluid velocity $u_1(\eta,\tau)$ is obtained and is expressed in the following form

$$\theta(\eta,\tau)=\theta_2(\eta,\tau)-\theta_2(\eta,\tau-1)H(\tau-1), \quad (24)$$

$$\begin{aligned}u_1(\eta,\tau)=\frac{1}{2}\Bigg[&e^{\frac{\eta}{\sqrt{MaDa}}}\operatorname{erfc}\left(\frac{\eta}{2\sqrt{\tau}}+\sqrt{\frac{\tau}{MaDa}}\right)\\&+e^{-\frac{\eta}{\sqrt{MaDa}}}\operatorname{erfc}\left(\frac{\eta}{2\sqrt{\tau}}-\sqrt{\frac{\tau}{MaDa}}\right)\Bigg]\\&-\gamma\left[\phi_2(\eta,\tau)-\phi_2(\eta,\tau-1)H(\tau-1)\right],\end{aligned} \quad (25)$$

where

$$\begin{aligned}\theta_2(\eta,\tau)=\frac{1}{2}\Bigg[&\left(\tau+\frac{\eta}{2\sqrt{Ra}}\right)e^{\eta\sqrt{Ra}}\operatorname{erfc}\left(\frac{\eta}{2\sqrt{\tau}}+\sqrt{Ra\tau}\right)\\&+\left(\tau-\frac{\eta}{2\sqrt{Ra}}\right)e^{-\eta\sqrt{Ra}}\operatorname{erfc}\left(\frac{\eta}{2\sqrt{\tau}}-\sqrt{Ra\tau}\right)\Bigg],\end{aligned} \quad (26)$$

$$\begin{aligned}\phi_2(\eta,\tau)=\frac{1}{2}\Bigg[&\left(\tau+\frac{\eta}{2\sqrt{Ra}}\right)e^{\eta\sqrt{Ra}}\operatorname{erfc}\left(\frac{\eta}{2\sqrt{\tau}}+\sqrt{Ra\tau}\right)\\&+\left(\tau-\frac{\eta}{2\sqrt{Ra}}\right)e^{-\eta\sqrt{Ra}}\operatorname{erfc}\left(\frac{\eta}{2\sqrt{\tau}}-\sqrt{Ra\tau}\right)\\&-\left(\tau+\frac{\eta\sqrt{MaDa}}{2}\right)e^{\frac{\eta}{\sqrt{MaDa}}}\operatorname{erfc}\left(\frac{\eta}{2\sqrt{\tau}}+\sqrt{\frac{\tau}{MaDa}}\right)\\&-\left(\tau-\frac{\eta\sqrt{MaDa}}{2}\right)e^{-\frac{\eta}{\sqrt{MaDa}}}\operatorname{erfc}\left(\frac{\eta}{2\sqrt{\tau}}-\sqrt{\frac{\tau}{MaDa}}\right)\Bigg],\end{aligned}$$

and $\gamma=Gr\Big/\left(Ra-\frac{1}{MaDa}\right)$.

2.2. Solution for Isothermal Case

In order to highlight the effects of the ramped temperature distribution near a vertical plate, it may be important to compare the effects of the isothermal temperature distribution for the fluid flow. The temperature and the velocity for the fluid flow near an isothermal plate can be expressed as

$$\begin{aligned}\theta(\eta,\tau)=\frac{1}{2}\Bigg[&e^{\eta\sqrt{\Pr Ra}}\operatorname{erfc}\left(\frac{\eta}{2}\sqrt{\frac{\Pr}{\tau}}+\sqrt{Ra\tau}\right)\\&+e^{-\eta\sqrt{\Pr Ra}}\operatorname{erfc}\left(\frac{\eta}{2}\sqrt{\frac{\Pr}{\tau}}-\sqrt{Ra\tau}\right)\Bigg],\end{aligned} \quad (27)$$

$$u_1(\eta,\tau)=\left[\frac{1}{2}e^{\frac{\eta}{\sqrt{MaDa}}}\operatorname{erfc}\left(\frac{\eta}{2\sqrt{\tau}}+\sqrt{\frac{\tau}{MaDa}}\right)\right.$$
$$\left.+e^{-\frac{\eta}{\sqrt{MaDa}}}\operatorname{erfc}\left(\frac{\eta}{2\sqrt{\tau}}-\sqrt{\frac{\tau}{MaDa}}\right)\right] \quad (28)$$
$$-\alpha\left[u_{11}(\eta,\tau)-u_{12}(\eta,\tau)\right],$$

where

$$u_{11}(\eta,\tau)=\frac{1}{2\beta}\left[e^{\beta\tau}\left\{e^{\eta\sqrt{\beta+\frac{1}{MaDa}}}\right.\right.$$
$$\times\operatorname{erfc}\left(\frac{\eta}{2\sqrt{\tau}}+\sqrt{\left(\beta+\frac{1}{MaDa}\right)\tau}\right)$$
$$\left.+e^{-\eta\sqrt{\beta+\frac{1}{MaDa}}}\operatorname{erfc}\left(\frac{\eta}{2\sqrt{\tau}}-\sqrt{\left(\beta+\frac{1}{MaDa}\right)\tau}\right)\right\}$$
$$-\left\{e^{\frac{\eta}{\sqrt{MaDa}}}\operatorname{erfc}\left(\frac{\eta}{2\sqrt{\tau}}+\sqrt{\frac{\tau}{MaDa}}\right)\right.$$
$$\left.\left.+e^{-\frac{\eta}{\sqrt{MaDa}}}\operatorname{erfc}\left(\frac{\eta}{2\sqrt{\tau}}-\sqrt{\frac{\tau}{MaDa}}\right)\right\}\right]$$

$$u_{12}(\eta,\tau)=\frac{1}{2\beta}\left[e^{\beta\tau}\left\{e^{\eta\sqrt{(\beta+Ra)\Pr}}\right.\right.$$
$$\times\operatorname{erfc}\left(\frac{\eta}{2}\sqrt{\frac{\Pr}{\tau}}+\sqrt{(\beta+Ra)\tau}\right)$$
$$\left.+e^{-\eta\sqrt{(\beta+Ra)\Pr}}\operatorname{erfc}\left(\frac{\eta}{2}\sqrt{\frac{\Pr}{\tau}}-\sqrt{(\beta+Ra)\tau}\right)\right\}$$
$$-\left\{e^{\eta\sqrt{\Pr Ra}}\operatorname{erfc}\left(\frac{\eta}{2}\sqrt{\frac{\Pr}{\tau}}+\sqrt{Ra\tau}\right)\right. \quad (29)$$
$$\left.\left.+e^{-\eta\sqrt{\Pr Ra}}\operatorname{erfc}\left(\frac{\eta}{2}\sqrt{\frac{\Pr}{\tau}}-\sqrt{Ra\tau}\right)\right\}\right].$$

When $\Pr=1$, the Solutions (27) and (28) become

$$\theta(\eta,\tau)=\frac{1}{2}\left[e^{\eta\sqrt{Ra}}\operatorname{erfc}\left(\frac{\eta}{2\sqrt{\tau}}+\sqrt{Ra\tau}\right)\right.$$
$$\left.+e^{-\eta\sqrt{Ra}}\operatorname{erfc}\left(\frac{\eta}{2\sqrt{\tau}}-\sqrt{Ra\tau}\right)\right], \quad (30)$$

$$u_1(\eta,\tau)=u_{13}(\eta,\tau)+\gamma\left[u_{13}(\eta,\tau)-u_{14}(\eta,\tau)\right], \quad (31)$$

where

$$u_{13}(\eta,\tau)=\frac{1}{2}\left[e^{\frac{\eta}{\sqrt{MaDa}}}\operatorname{erfc}\left(\frac{\eta}{2\sqrt{\tau}}+\sqrt{\frac{\tau}{MaDa}}\right)\right.$$
$$\left.+e^{-\frac{\eta}{\sqrt{MaDa}}}\operatorname{erfc}\left(\frac{\eta}{2\sqrt{\tau}}-\sqrt{\frac{\tau}{MaDa}}\right)\right], \quad (32)$$

$$u_{14}(\eta,\tau)=\frac{1}{2}\left[e^{\eta\sqrt{Ra}}\operatorname{erfc}\left(\frac{\eta}{2\sqrt{\tau}}+\sqrt{Ra\tau}\right)\right.$$
$$\left.+e^{-\eta\sqrt{Ra}}\operatorname{erfc}\left(\frac{\eta}{2\sqrt{\tau}}-\sqrt{Ra\tau}\right)\right]. \quad (33)$$

3. Results and Discussion

We have plotted the non-dimensional velocity and temperature for several values of radiation parameter Ra, Prandtl number $\Pr$, Grashof number Gr, Darcy number Da and time τ in **Figures 2-9**. **Figures 2-6** represent the velocity u_1 against η for several values of Ra, $\Pr$, Gr, Da and τ. **Figure 2** shows that an increase in the radiation parameter Ra leads to fall in the velocity u_1 for both ramped wall temperature as well as isothermal wall temperature. **Figure 3** displays that the velocity u_1 decreases for both ramped wall temperature as well as isothermal wall temperature with an increase in Prandtl number $\Pr$. Physically, this is true because the increase in the Prandtl number is due to increase in the viscosity of the fluid which makes the fluid thick and hence causes a decrease in the velocity of the fluid. It is observed from **Figure 4** that an increase in Gr, leads to a rise in the values of velocity u_1 due to enhancement in buoyancy force. **Figure 5** reveals that the velocity u_1 increases for both ramped wall temperature as well as isothermal wall temperature with an increase in Darcy number Da. It is seen from **Figure 6** that the velocity u_1 increases for both ramped wall temperature as well as isothermal wall temperature with an increase in time τ. It is observed from **Figure 7** that the temperature θ decreases as the radiation parameter Ra increases for both ramped wall temperature as well as isothermal wall temperature. This result qualitatively agrees with expectations, since the effect of radiation is to decrease the rate of energy transport to the fluid, thereby decreasing the temperature of the fluid. It is seen from **Figure 8** that the temperature θ decreases for both ramped wall temperature as well as isothermal wall temperature with an increase in Prandtl number $\Pr$. This implies that an increase in Prandtl number leads to fall the thermal boundary layer flow for ramped temperature as well as isothermal wall temperature. The effect of the Prandtl number is very important in the temperature field. A fall in temperature occurs due to an increasing value of the Prandtl number. This is in agreement with the physical fact that the thermal boundary layer thickness decreases with increase in $\Pr$. **Figure 9**

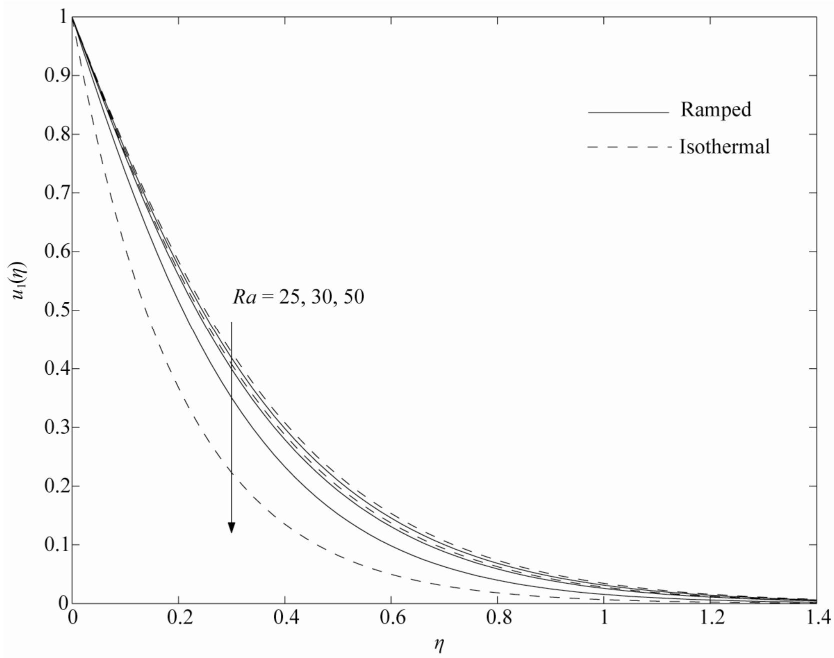

Figure 2. Velocity profiles for variations in Ra when $\Pr = 0.71$, $Gr = 25$, $\tau = 0.1$ and $Da = 0.04$.

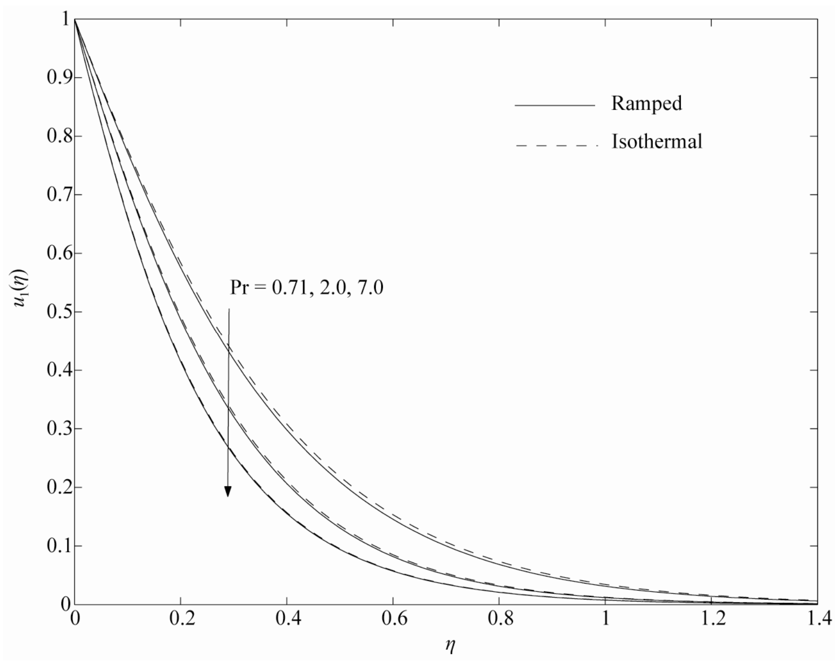

Figure 3. Velocity profiles for variations in Pr when $Da = 0.04$, $Gr = 25$, $\tau = 0.1$ and $Ra = 2$.

shows that the temperature θ increases for both ramped wall temperature as well as isothermal wall temperature with an increase in time τ.

From the physical point of view, it is necessary to know the shear stress and the rate of heat transfer (or the Nusselt number) at the wall $(\eta = 0)$. We have presented the expression for the rate of heat transfer Nu and shear stress τ_0 at the wall $\eta = 0$ in the following form for both the ramped wall temperature and isothermal wall temperature.

For the ramped wall temperature

$$Nu = -\frac{\partial \theta}{\partial \eta}\bigg]_{\eta=0} = \theta_3(\eta,\tau) - \theta_3(\eta,\tau-1)H(\eta-1), \quad (34)$$

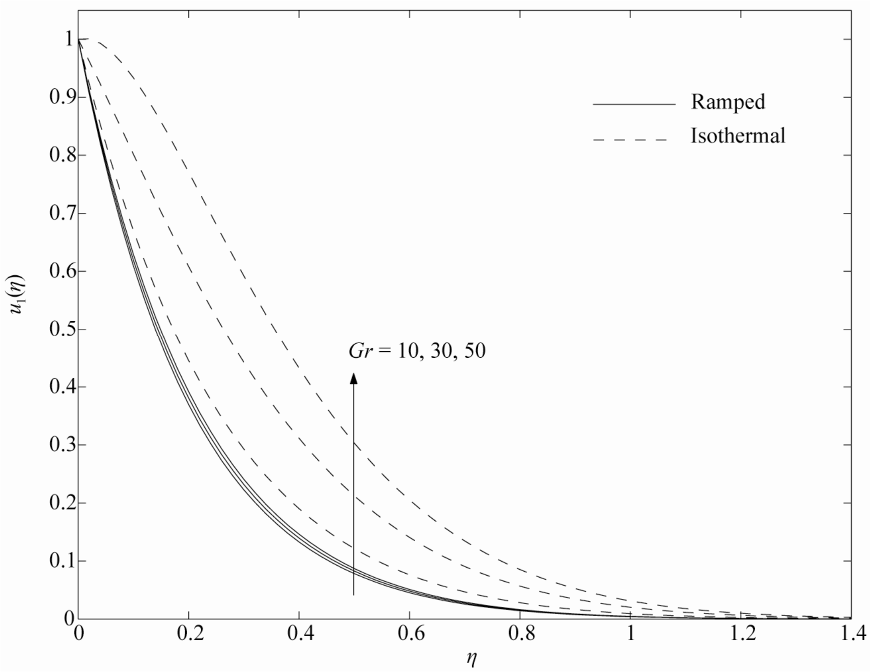

Figure 4. Velocity profiles for variations in Gr when $\Pr = 0.71$, $Da = 0.04$, $\tau = 0.1$ and $Ra = 2$.

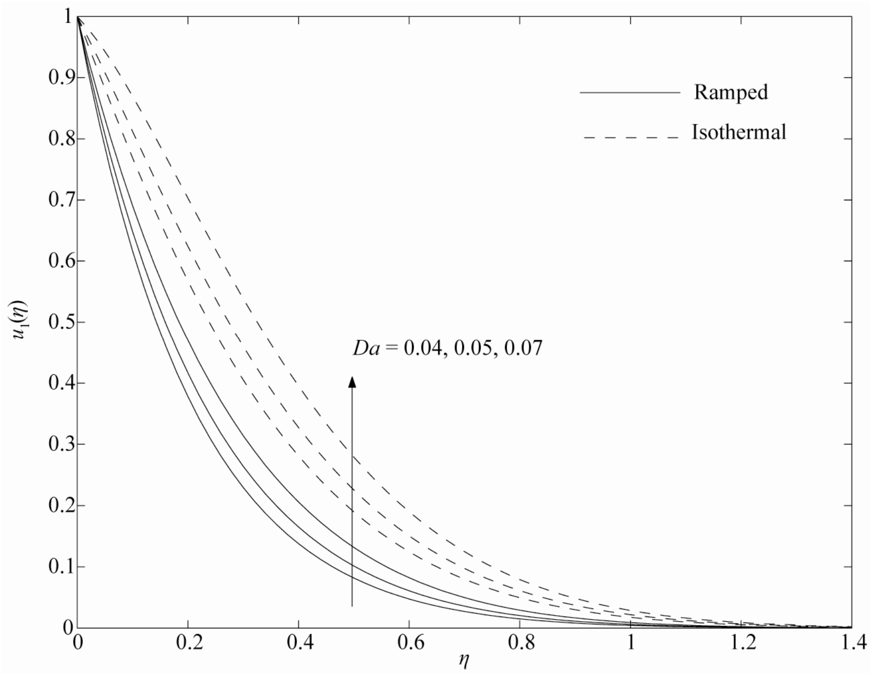

Figure 5. Velocity profiles for variations in Da when $\Pr = 0.71$, $Gr = 25$, $\tau = 0.1$ and $Ra = 2$.

$$\tau_0 = \frac{\partial u_1}{\partial \eta}\bigg]_{\eta=0} = -\left[\frac{1}{\sqrt{\pi\tau}}e^{-\frac{\tau}{MaDa}} + \sqrt{\frac{1}{MaDa}}\operatorname{erf}\left(\sqrt{\frac{\tau}{MaDa}}\right)\right] - \alpha\left[\phi_3(\eta,\tau) - \phi_3(\eta,\tau-1)H(\eta-1)\right], \tag{35}$$

where

$$\phi_3(\eta,\tau) = -\frac{e^{\beta\tau}}{\beta^2}\left\{\sqrt{\frac{1}{MaDa}+\beta}\operatorname{erf}\left(\sqrt{\left(\frac{1}{MaDa}+\beta\right)\tau}\right) + \frac{1}{\sqrt{\pi\tau}}e^{-\left(\frac{1}{MaDa}+\beta\right)\tau} - \sqrt{\Pr(Ra+\beta)}\operatorname{erf}\left(\sqrt{(Ra+\beta)\tau}\right)\right.$$

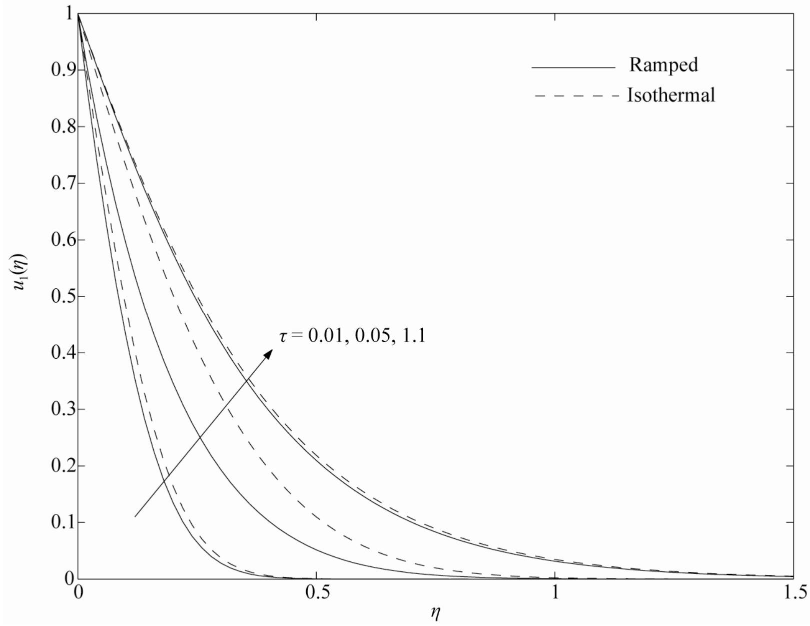

Figure 6. Velocity profiles for variations in time τ when $\mathrm{Pr} = 0.71$, $Gr = 25$, $Ra = 2$ and $Da = 0.04$.

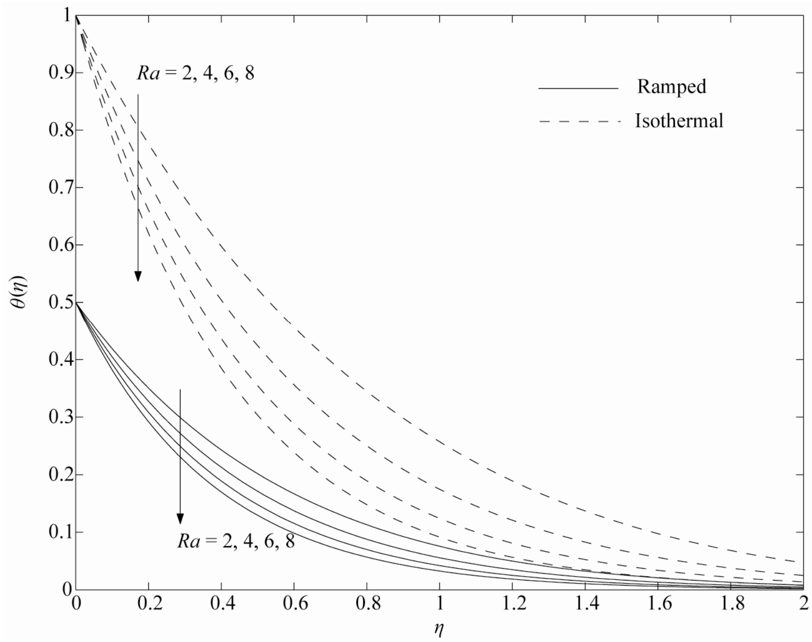

Figure 7. Temperature profiles for variations in Ra when $\mathrm{Pr} = 0.71$ and $\tau = 0.5$.

$$-\sqrt{\frac{\mathrm{Pr}}{\pi\tau}}e^{-(Ra+\beta)\tau}\Bigg\}+\frac{1}{\beta}\Bigg\{\frac{\sqrt{MaDa}}{2}\mathrm{erf}\left(\sqrt{\frac{\tau}{MaDa}}\right)$$

$$+\frac{1}{\sqrt{MaDa}}\left(\tau+\frac{1}{\beta}\right)\mathrm{erf}\left(\sqrt{\frac{\tau}{MaDa}}\right)$$

$$+\frac{1}{\sqrt{\pi\tau}}\left(\tau+\frac{1}{\beta}\right)e^{-\frac{\tau}{MaDa}}\Bigg\}-\frac{1}{\beta}\Bigg\{\frac{1}{2}\sqrt{\frac{\mathrm{Pr}}{Ra}}\mathrm{erf}\left(\sqrt{Ra\tau}\right)$$

$$+\sqrt{\mathrm{Pr}\,Ra}\left(\tau+\frac{1}{\beta}\right)\mathrm{erf}\left(\sqrt{Ra\tau}\right)+\sqrt{\frac{\mathrm{Pr}}{\pi\tau}}\left(\tau+\frac{1}{\beta}\right)e^{-Ra\tau}\Bigg\}, \tag{36}$$

and for the isothermal wall temperature

$$Nu=-\frac{\partial\theta}{\partial\eta}\Bigg]_{\eta=0}=\sqrt{\mathrm{Pr}\,Ra}\,\mathrm{erf}\left(\sqrt{Ra\tau}\right)+\sqrt{\frac{\mathrm{Pr}}{\pi\tau}}e^{-Ra\tau}, \tag{37}$$

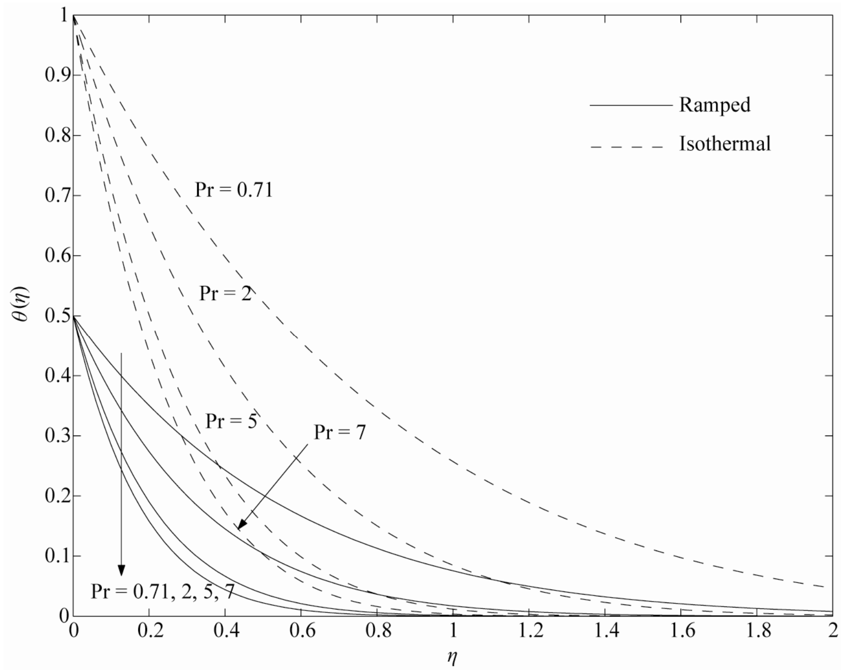

Figure 8. Temperature profiles for variations in Pr when $Ra = 2$ and $\tau = 0.5$.

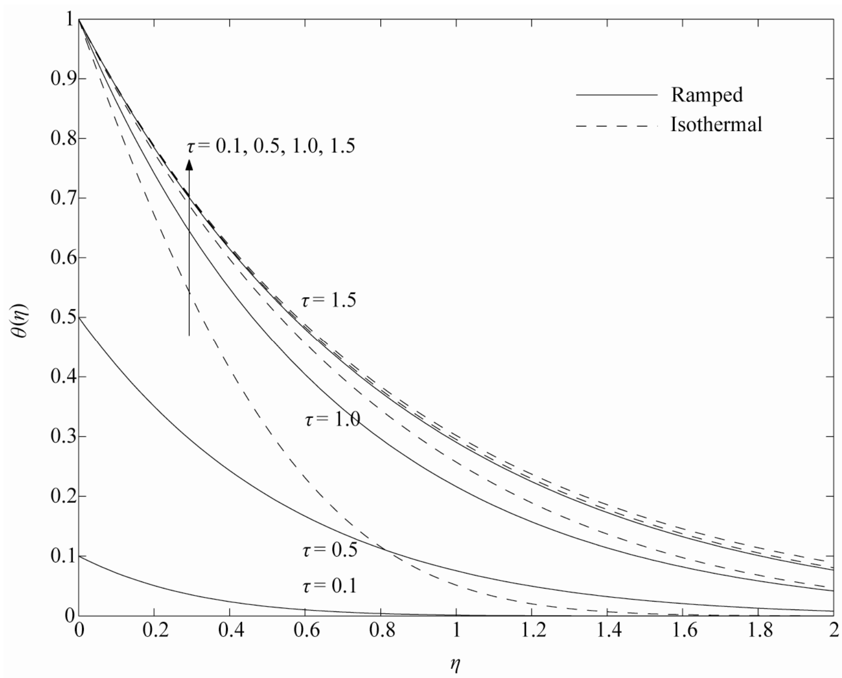

Figure 9. Temperature profiles for variations in time τ when $\Pr = 0.71$ and $Ra = 2$.

$$\tau_0 = \left.\frac{\partial u_1}{\partial \eta}\right]_{\eta=0} = -\Bigg[\left(1+\frac{\alpha}{\beta}\right)\frac{1}{\sqrt{MaDa}}\operatorname{erf}\left(\sqrt{\frac{\tau}{MaDa}}\right) + \frac{1}{\sqrt{\pi\tau}}e^{-\frac{\tau}{MaDa}} + \frac{\alpha}{\beta}\Bigg\{e^{\beta\tau}\sqrt{\Pr\left(Ra+\beta\right)}\operatorname{erf}\left(\sqrt{\left(Ra+\beta\right)\tau}\right) - e^{\beta\tau}\sqrt{\frac{1}{MaDa}+\beta}\operatorname{erf}\left(\sqrt{\left(\frac{1}{MaDa}+\beta\right)\tau}\right) - \sqrt{\Pr Ra}\operatorname{erf}\left(\sqrt{Ra\tau}\right)\Bigg\}\Bigg]. \quad (38)$$

Numerical results of shear stress at the wall $(\eta = 0)$ are presented in **Tables 1** to **4** for various values radiation parameter Ra, Prandtl number $\Pr$, Grashof number $Gr = 4$, Darcy number Da and time τ. **Table 1** shows that the magnitude of shear stress τ_0 decreases for both ramped wall temperature as well as isothermal wall temperature with an increase in Darcy number Da for fixed values of Ra and while the result is reversed with an increase in radiation parameter Ra for fixed values of Da. It is observed from **Table 2** that the magnitude of shear stress τ_0 decreases for both ramped wall temperature as well as isothermal wall temperature with increase in either Darcy number Da or Grashof nubmer Gr. It is also observed from **Table 3** that the magnitude of shear stress τ_0 decreases for both ramped wall temperature as well as isothermal wall temperature with an increase in time τ. **Table 4** displays that for creases for both ramped wall temperature as well as isothermal wall temperature with an increase in Prandtl number $\Pr$.

Table 1. Shear stress $-\tau_0$ for $\Pr = 0.71$, $Gr = 10$ and $\tau = 1$.

	Ramped temperature			Isothermal temperature		
Da/Ra	25	30	35	25	30	35
0.040	3.93632	3.97912	4.01576	3.91459	3.95998	3.99849
0.045	3.61771	3.66324	3.70195	3.59386	3.64215	3.68301
0.050	3.34675	3.39462	3.43524	3.32075	3.37170	3.41473
0.055	3.11244	3.16245	3.20487	3.08436	3.13779	3.18282

Table 2. Shear stress $-\tau_0$ for $\Pr = 0.71$, $Ra = 25$ and $\tau = 1$.

	Ramped temperature			Isothermal temperature		
Da/Gr	10	15	20	10	15	20
0.040	3.9363	3.4044	2.8726	3.91459	3.37188	2.82917
0.045	3.6177	3.0696	2.5214	3.59386	3.03377	2.47368
0.050	3.3467	2.7840	2.2214	3.32075	2.74506	2.16937
0.055	3.1124	2.5366	1.9608	3.08436	2.49454	1.90471

Table 3. Shear stress $-\tau_0$ for $\Pr = 0.71$ and $Gr = 10$.

	Ramped temperature			Isothermal temperature		
τ/Ra	25	30	35	25	30	35
0.5	4.93191	4.93417	4.93632	3.96181	4.00034	4.03430
1.0	4.80524	4.81177	4.81752	3.91696	3.96170	3.99986
1.5	4.69611	4.70716	4.71677	3.91474	3.96007	3.99855
2.0	4.58754	4.60313	4.61657	3.91460	3.95998	3.99849

Table 4. Shear stress $-\tau_0$ for $Ra = 25$, $Da = 0.4$.

	Ramped temperature			Isothermal temperature		
$\Pr/\tau$	0.5	1.0	1.5	0.5	1.0	1.5
0.71	4.93191	4.80524	4.69611	3.96181	3.91696	3.91474
2.0	4.95270	4.85151	4.76807	4.21229	4.17355	4.17170
5.0	4.96972	4.88940	4.82698	4.41735	4.38361	4.38207
7.0	4.97534	4.90190	4.84643	4.48504	4.45295	4.45151

Numerical results of the rate of heat transfer at the $(\eta = 0)$ are presented in **Tables 5** to **6** for various values radiation parameter Ra, Prandtl number $\Pr$ and time τ. **Table 5** shows that the rate of heat transfer Nu increases for both ramped wall temperature as well as isothermal wall temperature with an increase in radiation parameter Ra. Further, the rate of heat transfer increases for ramped wall temperature while it decreases isothermal wall temperature with an increase in time τ for fixed values of Ra. It is observed from **Table 6** that for fixed value of time τ, the rate of heat transfer Nu increases for both ramped wall temperature as well as for isothermal wall temperature with an increase in Prandtl number $\Pr$.

4. Conclusions

An analysis is made to study the radiation effects on free convection flow past an impulsively started infinite vertical wall with ramped wall temperature in a porous medium. The velocity field and temperature distribution are presented for different physical parameters graphically. It is observed that the velocity profiles decrease with an increase in Prandtl number $\Pr$ for ramped wall temperature as well as isothermal wall temperature. An increase in Grashof number Gr leads to a rise in the values of velocity due to enhancement in buoyancy force. The velocity field is accelerated due to increase in Darcy number Da. The effect of the Prandtl number is very important in the temperature field. A fall in temperature occurs due to an increasing value of the Prandtl number. It is found that the temperature decreases as the radiation parameter increases for both ramped wall temperature as well as isothermal wall temperature. Further, the absolute value of shear stress τ_0 increases for both ramped wall

Table 5. Rate of heat transfer $-Nu$ for $\Pr = 0.71$.

	Ramped temperature			Isothermal temperature		
Ra/τ	0.1	0.2	0.3	0.1	0.2	0.3
2	0.32032	0.47976	0.61917	1.79436	1.46199	1.34228
4	0.33924	0.53046	0.70774	2.06757	1.81588	2.08819
6	0.35748	0.57787	0.78852	2.32489	2.13371	2.91893
8	0.37509	0.62246	0.86297	2.56804	2.42239	2.39419

Table 6. Rate of heat transfer $-Nu$ for $Ra = 25$.

	Ramped temperature			Isothermal temperature		
$\Pr/\tau$	0.1	0.2	0.3	0.1	0.2	0.3
0.71	0.32032	0.47976	0.61917	1.79436	1.46199	1.34228
2.0	0.53761	0.80520	1.03919	3.01159	2.45375	2.25283
5.0	0.85004	1.27314	1.64310	4.76174	3.87972	3.56204
7.0	1.00578	1.50640	1.94414	5.63417	4.59055	4.21466

temperature as well as isothermal wall temperature with an increase in Darcy number Da for fixed values of Ra and while the result is reversed with an increase in radiation parameter Ra for fixed values of Da. The rate of heat transfer Nu increases for both ramped wall temperature as well as isothermal wall temperature with an increase in radiation parameter Ra.

5. References

[1] P. S. Ghoshdastidar, "Heat Transfer," Oxford University Press, Oxford, 2004.

[2] D. A. Nield and A. Bejan, "Convection in Porous Media," Springer, New York, 2006, pp. 94-97.

[3] M. A. Mansour, "Radiation and Free Convection Effects on the Oscillating Flow past a Vertical Plate," *Astrophysics and Space Science*, Vol. 166, No. 2, 1990, pp. 269-275. doi:10.1007/BF01094898

[4] A. Raptis and C. Perdikis, "Radiation and Free Convection Flow past a Moving Plate," *Applied Mechanics and Engineering*, Vol. 4, No. 4, 1999, pp. 817-821.

[5] U. N. Das, R. Deka and V. M. Soundalgekar, "Radiation Effect on Flow past an Impulsively Started Vertical Plate: An Exact Solutions," *Journal of Applied Mathematics and Fluid Mechanics*, Vol. 1, No. 2, 1966, pp. 111-115.

[6] R. Grief, I. S. Habib and J. C. Lin, "Laminar Convection of Radiating Gas in a Vertical Channel," *Journal of Fluid Mechanics*, Vol. 46, 1991, pp. 513-520. doi:10.1017/S0022112071000673

[7] P. Ganesan and P. Loganathan, "Radiation and Mass Transfer Effects on Flow of an Incompressible Viscous Fluid past a Moving Vertical Cylinder," *International Journal of Heat and Mass Transfer*, Vol. 45, No. 21, 2002, pp. 4281-4288. doi:10.1016/S0017-9310(02)00140-0

[8] I. U. Mbeledogu, A. R. C. Amakiri and A. Ogulu, "Unsteady MHD Free Convection Flow of a Compressible Fluid past a Moving Vertical Plate in the Presence of Radiative Heat Transfer," *International Journal of Heat and Mass Transfer*, Vol. 50, No. 9-10, 2007, pp. 326-331. doi:10.1016/j.ijheatmasstransfer.2006.10.032

[9] O. D. Makinde, "Free-Convection Flow with Thermal Radiation and Mass Transfer past a Moving Vertical Porous Plate," *International Communications in Heat and Mass Transfer*, Vol. 32, No. 10, 2005, pp. 1411-1419. doi:10.1016/j.icheatmasstransfer.2005.07.005

[10] M. D. Abdus-Sattar and M. D. Hamid Kalim, "Unsteady Free-Convection Intraction with Thermal Radiation in a Boundary Layer Flow past a Vertical Porous Plate," *Journal of Mathematical Physics*, Vol. 30, 1996, pp. 25-37.

[11] C. Israel-Cookey, A. Ogulu and V. B. Omubo-Pepple, "Influence of Viscous Dissipation and Radiation on Unsteady MHD Free-Convection Flow past an Infinite Heated Vertical Plate in a Porous Medium with Time-Dependent Suction," *International Journal of Heat and Mass Transfer*, Vol. 46, No. 13, 2003, pp. 2305-2311. doi:10.1016/S0017-9310(02)00544-6

[12] K. D. Alagoa, G. Tay and T. M. Abbey, "Radiative and Free Convective Effects of a MHD Flow through a Porous Medium between Infinite Parallel Plates with Time-Dependent Suction," *Astrophysics and Space Science*, Vol. 260, 1999, pp. 455-468. doi:10.1016/S0017-9310(02)00544-6

[13] C. Israel-Cookey, E. Amos and C. Nwaigwe, "MHD Oscillatory Couette Flow of a Radiating Viscous Fluid in a Porous Medium with Periodic Wall Temperature," *American Journal of Scientific and Industrial Research*, Vol. 1, No. 2, 2010, pp. 326-331. doi:10.5251/ajsir.2010.1.2.326.331

[14] M. A. Sattar and M. A. Maleque, "Unsteady MHD Natural Convection Flow along an Accelerated Porous Plate with Hall Current and Mass Transfer in a Rotating Porous Medium," *Journal of Energy*, *Heat and Mass Transfer*, Vol. 22, 2000, pp. 67-72.

[15] M. A. Sattar, M. M. Rahman and M. M. Alam, "Free Convection Flow and Heat Transfer through a Porous Vertical Flat Plate Immersed in a Porous Medium," *Journal of Energy Research*, Vol. 22, No. 1, 2000, pp. 17-21.

[16] M. D. Abdus Samad and M. Mansur Rahman, "Thermal Radiation Interaction with Unsteady MHD Flow past a Vertical Porous Plate Immersed in a Porous Medium," *Journal of Naval Architecture and Marine Engineering*, Vol. 3, No. 1, 2006, pp. 7-14.

[17] N. C. Mahanti and P. Gaur, "The Effects of Varying Viscosity and Thermal Conductivity on Steady Free Convective Flow and Heat Transfer along an Isothermal Vertical Plate in the Presence of Heat Sink," *Journal of Applied Fluid Mechanics*, Vol. 2, No. 1, 2009, pp. 23-28.

[18] H. S. Takhar, P. Ganesan, K. Ekambavanan and V. M. Soundalgekar, "Transient Free Convection past a Semi Infinite Vertical Plate with Variable Surface Temperature," *International Journal of Numerical Methods for Heat and Fluid Flow*, Vol. 7, No. 4, 1997, pp. 280-296. doi:10.1108/09615539710165804

[19] A. C. L. Cogley, W. G. Vincenti and E. S. Gilles, "Differential Approximation for Radiative Heat Transfer in a Non Grey Gas near Equilibrium," *American Institute of Aeronautics and Astronautics*, Vol. 6, No. 3, 1968, pp. 551-553.